

Electromigration-Aware Architecture for Modern Microprocessors

Freddy Gabbay and Avi Mendelson, *Fellow, IEEE*

Abstract— Reliability is a fundamental requirement in microprocessors to guarantee correct execution over their lifetime. The reliability related design rules depend on the process technology and the device operating conditions. To meet reliability requirements, advanced technologies impose challenging design rules which have become a major burden on the VLSI implementation flow because of the severe physical constraints they impose. This paper focuses on electromigration (EM), which is one of the critical factors affecting semiconductor reliability. EM is the aging process of on-die wires which is induced by excessive current flow that can damage wires in integrated-circuits. EM exerts a comprehensive global effect on devices because it impacts wires inside logical cells, between cells, inside memory elements, and within wires that interconnect functional blocks. Traditionally, reliability and EM issues have been handled at the physical design level that enforces reliability rules using worst case scenario analysis in order to detect and solve violations. Contrarily, this study proposes EM-aware microarchitectural solution that can significantly relax the over-design of the traditional methods and to extend products lifetime. Our results show that with minimal area, power and performance overhead, the new proposed solution can relax EM design efforts and more than double microprocessor lifetime.

Index Terms— Electromigration, Reliability, Electromigration-aware architecture

I. INTRODUCTION

CHIP reliability is an essential design requirement and is crucial to assure the correct functionality of a semiconductor integrated circuit (IC). For every product, chip vendors are required to guarantee a minimum lifetime, which depends on a reliability prediction for each chip. To meet these reliability requirements, a design-for-reliability methodology was developed that, unfortunately, is highly complicated because it depends on the expected workload, the process technology, the operating voltage, and the temperature. As part of the design-for-reliability methodology of modern processors, a workflow is defined [1,2,3] that aims to guarantee a minimum product lifetime under a specified workload (i.e., the mission profile). Given the use of new advanced process technologies and new applications such as computation-intensive infrastructures (e.g., autonomous cars, datacenter and cloud computing, life-support systems, etc.), the need for high

reliability has recently heightened.

The shrinking dimensions of VLSI technology, the increasing density of logical elements, and the challenging voltage and temperature operating conditions combine today to make electromigration (EM) one of the most influential factors affecting the reliability of modern systems. EM is a phenomenon related to the reliability of wires and vias in ICs and is caused by excessive current flow that can potentially damage a physical device. Such damage may either reduce a wire's conductivity or cause wire disconnect, both of which lead to reliability concerns. In this work, we focus on the impact of EM on wires and vias that reside inside logical cells or memory elements; or used as interconnects between logical cells or functional units.

To date, the design community has focused on enhancing chip-design implementation flow [1,2,4-10] to solve EM issues, whereas few works have proposed architectural solutions. In this study, we propose a novel architecture that significantly improves reliability by reducing EM impact while relaxing the physical design efforts and significantly extending microprocessor lifetime. This study is based on the observation that numerous EM reliability concerns result from excessive write activities (or change of logical state) spread across processing elements of the same type (gates, logical units, or memory elements) in a nonuniform manner. This observation led us to develop enhanced resource-allocation mechanisms that uniformly distribute the write operations workload across all resources. As a result, the maximum EM stress induced by singular elements is minimized, and the overall IC reliability is extended in up to several orders of magnitude. Our study also enhances conventional EDA (electronic-design-automation) tools which suffer from lack of architectural information on the toggle rate of the analyzed circuit and often assume a worst-case toggling rate that may result in over design and shorter device lifetime. This work focuses on a microprocessor as a case study; however, the concepts can be applied to other ICs and applications.

The remainder of this paper is organized as follows: Section 2 introduces EM reliability challenges and reviews EM and previous works. Section 3 introduces the limitations of modern microprocessor to deal EM, Section 4 describes the proposed EM-aware microarchitectural enhancements, and Section 5

This paper was submitted for a review on August 4th, 2020.

F. Gabbay. Author is with the Electrical Engineering Department, Ruppin Academic Center, Israel (e-mail: freddyg@ruppin.ac.il).

A. Mendelson. Author is with the Computer Science and Electrical Engineering Departments, Technion – Israel Institute of Technology of Technology, Haifa, Israel 3200000 Israel (e-mail: avi.mendelson@technion.ac.il).

presents simulation results of the proposed EM-aware microarchitecture. Finally, Section 6 summarizes the study and suggests future works.

II. IC RELIABILITY

IC reliability has become a crucial discipline in VLSI chip design. The need for highly reliable systems has existed from the early days of computing and was mainly driven in the past by “special systems” such as mission-critical embedded systems. However, given the vulnerability of the new process technology and the appearance of new applications that require safe and reliable processing such as autonomous cars, large-scale computing-intensive systems, and life-support systems, reliability today is a fundamental requirement for most systems. The product specifications of such systems impose strict requirements on reliability through the lifetime and operating conditions. For example, the automotive industry expects an IC to function reliably for 10–15 years at a given temperature (usually about 125 °C [11,12] and under various workloads. In data-center computing, the requirements are slightly relaxed but remain challenging: the lifetime requirement demands at least ten years, whereas the temperature can range from 105 to 110 °C with arbitrary workloads. None of these reliability-sensitive applications can afford microprocessor faults caused by reliability issues.

Over the past decade, as advanced process technologies have been introduced, the susceptibility to reliability-related issues has grown dramatically. Starting at 28 nm process technology and below, the design efforts dedicated to reliability have substantially increased. The design community has mainly tried to enhance the synthesis and place-and-route flows to handle reliability-related issues. Such flows involve substantial design efforts and, in many cases, required multiple iterations to make the IC comply with the design rules (also known as the “sign-off process”). Note that few prior studies have addressed these reliability challenges from the architecture point of view [5–8]. The remainder of this section reviews the EM phenomenon and previous related studies.

A. Electromigration

EM is a physical phenomenon related to excessive current density within wires and vias. EM became a major concern in advanced process technologies when the geometrical dimension of wires and vias shrank to very small dimensions, making them highly susceptible to the negative effect of electrical current stress. This stress is induced by the force of conduction electrons and metal ions. When the force of conduction electrons reaches a certain strength level, it may tear atoms from the boundary of the metal and transport them in the direction of the current flow. If such current force is maintained for a long time or if current flows frequently, the wire may become malformed. To ease the problem, one may consider occasionally reversing the current direction, but experiments indicate that such a strategy has minor impact on improving on the overall reliability issues (e.g., wire disconnect or significant change in the wire resistance). The occurrence of such an issue, even on a single wire, may result in overall chip failure. Note

also that the geometrical granularity of wires plays a major role in susceptibility to EM, with smaller wire granularity encouraging greater EM forces. Therefore, we expect EM to continue to be a major challenge in semiconductors as we deploy new advanced process nodes [8].

Black [13] derived the following formula for the EM mean time to failure (MTTF):

$$MTTF = \frac{A}{J^n} e^{\frac{E_a}{k_B T}}$$

Equation 1- EM MTTF

where A is a constant, J is the current density, E_a is the activation energy, n is a scaling factor, k_B is the Boltzmann constant, and T is the absolute temperature. The MTTF depends exponentially on temperature; in fact, higher temperature accelerates the negative effect of EM because it weakens the atomic bonds in a wire by making them even more sensitive to EM forces. Because many new applications, and in particular control systems (e.g., in the automotive or robotics fields), are required to operate at high temperatures of 105–125 °C, this induces much greater susceptibility to EM that will be highly challenging to mitigate during IC implementation and sign-off. In addition to the temperature effect, Refs. [6,14] express the current density J in metals as

$$J = \frac{CV_{DD}}{WH} pf$$

Equation 2 - Current Density

where C is the wire capacitance, W and H are the metal width and height, respectively, V_{DD} is the operating voltage, f is the clock frequency, and p is the switching probability, also known as the toggle rate. To meet the reliability requirements, two additional design-rule constraints are usually imposed by advanced process technology design rules [14]:

1. The current applied in every wire should be less than the peak current allowed by the process technology.
2. The current flow in a wire must be calculated by using the root mean square (RMS). Note that the use of an average current is not useful for EM analysis because the average current is usually zero since the number of charge carriers is the same when charging or discharging an electrical junction. More details on RMS current are available in Ref. [14].

For advanced process technologies, RMS current has become a very significant concern for EM reliability because of the incredibly small dimensions of wires and vias.

Handling the design rules for both maximum current and RMS current is highly challenging. The maximum-current constraint is mainly enforced by the physical design implementation tools that assure that the driving gates will not exceed the maximum-current limitation and by other physical design means [14]. With respect to the RMS current, the situation is more complex. Equation 2 shows that the RMS current flow within a wire is proportional to both the toggle rate and the clock frequency, which means that a higher toggle rate for logical elements increases the susceptibility to EM stress. Therefore, the MTTF of wires and vias can be increased either by increasing their physical width W or by minimizing their switching rate p. Increasing the wire width has, of course, a

negative impact on die area and on the number of available routing resources, which can degrade performance and increase overall power consumption. Minimizing the switching probability depends on both workload and architecture. In many cases, the switching probability depends on the change of logical state due to a write operation or to the use of logical elements for different computations. Read operation may also involve switching of wires state, however this usually happens on read ports shared between memory cells and therefore has smaller contribution to EM stress hotspots. Further studies on EM and its effects are available in Refs. [1,2,9,10,17,19]. To relax EM stress, we propose in Section IV a novel architectural solution that exploits the relationship between EM and toggle rate.

B. Prior Works on Electromigration

This subsection summarizes previous works on EM. The overview differentiates between works that propose EM solutions through the physical design flow and works that do so through micro-architectural or architectural solutions.

1) Prior work based on physical design

EM phenomena have been broadly studied from the physical design point of view. Various studies [4,7,16] examined different interconnects such as copper or aluminum and how they are affected by EM under different process, voltage, and temperature conditions. From a physical point of view, the most common solution for EM is to widen the wires. As Equation 2 indicates, this reduces the current density and eventually decreases the effect of EM but, from the physical design viewpoint, it is not always the preferred solution because it may introduce several over-heads, such as increasing the die area, which may reduce the device frequency. In addition, a larger die may also create timing and power challenges because signals would need to travel farther.

Modern electronic-design-automation (EDA) tool vendors, in conjunction with process foundries, enforce EM-related design rules as part of the IC sign-off process. Such tools verify that interconnects and vias meet the EM design rules and identify all EM-related violations that require design fixes. EM analysis tools are even able to simulate switching activity patterns extracted from functional simulations representing real applications and take these patterns into account in the EM analysis process. When the worst-case switching patterns cannot be determined, designers often use a statistical analysis provided by the EDA sign-off tool. In this case, the design is analyzed under a given set of switching probabilities, which may lead to an over-design process. The EM sign-off process is tedious and involves many fix iterations and trials. Some of the trials involve the use of wider metals and vias and, in several cases, may even limit the clock frequency, the switching rate, and the computational workload. The combination of all these limitations may result in degraded IC performance.

A study by Dasgupta et al. [7] introduced a methodology for synthesizing the design and scheduling data transfer from the control data flow graph to the hardware buses in an EM-aware manner. Their algorithm requires that the activity be determined in advance, so it becomes tightly coupled to each specific computational use that it targets.

A broad survey of additional physical-design-based techniques to mitigate EM impact is available in Ref. [10].

2) Prior work based on architecture

Only a limited number of prior works have suggested architecture-based solutions to the EM problem. Srinivasan et al. [6] suggested structural duplication and graceful performance degradation techniques to handle the EM effect. Structural duplication adds spare design structures to the IC and turns them on when the original structures fail. Graceful performance degradation, however, shuts down failing structures but keeps the IC functional while degrading its performance. This approach seems to incur a major hardware overhead related to the dedicated mechanisms to detect EM degradation through normal IC operation and the need for special circuits to switch on the redundant logic. In addition, it introduces extra power and performance overhead due to the addition of redundant hardware.

Abella et al. suggested [8] a novel architectural approach for “refueling” bi-directional busses by monitoring the current-flow direction each time data is transferred on the bus and suggested a mechanism that triggers current compensation whenever an imbalance occurs between the current flowing in each direction. Such a scheme could indeed relieve EM stress in older technologies; however, it has limited impact on advanced process nodes because the healing effect of RMS current is less effective, and its negative impact on wire and via reliability is more significant. In addition, given their design complexity, modern VLSI circuits do not commonly use bidirectional buses. The refueling mechanism also disrupts bus operation and may introduce a dynamic power overhead due to the reversal current.

Srinivasan et al. [5,20] suggested a dynamic reliability management approach where the processor dynamically maintains its lifetime reliability target by responding to the changing behavior of the application. This approach allows a processor with lower reliability to correctly operate while compromising performance or operating conditions.

Swaminathan et al. ([28]) introduced BRAVO, a cycle-accurate microprocessor simulation platform to assist designer and architects take into account reliability factors into consideration. Their tool can model voltage, energy and reliability to explore the optimal operating point for applications. EM impact is modeled using analytical means (Equation 1).

Based on all these evidences, we conclude that applying only physical design-based solutions does not suffice because of the growing challenges involved by EM. The remainder of this paper describes our comprehensive architectural solution for handling EM.

III. DISTRIBUTION OF ELECTROMIGRATION STRESS IN MODERN MICROPROCESSORS

By examining the arguments contributing to EM in Equation 1 and Equation 2 our main focus is the switching probability, P . This factor is tightly coupled to micro-architectural assumptions and application workload while all other

arguments are mainly related to process technology. It should also be noted, that current EM analysis tools extract the toggle rate without detailed analysis. This may lead to over-design, and therefore our analysis becomes valuable. In our study we assume that all other factors in these equations are constant due the following reasons: The junction temperature has indeed a major contribution to EM, however since it also depends on the workload and system cooling solution, common design flows usually consider the worst-case scenario of 105C or 125C in the sign-off process. As for metal width and height, the microprocessor blocks that we examine, such as ALUs, registers and memory elements, already utilize lower metal layers (typically metal 1-3) which are highly susceptible to EM. Upper metal layers are less susceptible and are mainly used for inter-block connectivity and power grid connections. We also assume operating at nominal voltage and do not assume power saving modes, such as DVS (dynamic voltage scaling), which can save power and decrease EM stress while reducing performance. Finally, the capacitance parameter depends on process intrinsic capacitance and wire length. The latter supports our interest in memories because they utilize long wires and hence are more susceptible to EM.

Since EM design rules are limited by the weakest link (i.e., the most susceptible wire), we start by examining the distribution of the switching probability over several sub-systems of a modern microprocessor which are expected to be highly susceptible to EM effect due to hot spots of toggling rate of wires. It should be noted that EM stress related to metal wires that are part of the IC power grid is out of the scope of this paper. Subsection A describes our experimental environment, and subsection B presents our comprehensive observations on EM stress in microprocessors.

A. Experimental Environment

Our experiments use the sniper x86-64 simulator [21]. We modified the simulation platform and added the needed mechanisms to model the behavior and measure the characteristics required for our experiments. The simulation environment includes both a detailed cycle-level x86 core model and a memory system. Table 1 summarizes the configuration of the simulation environment (based on the Intel Gainestown core [22]). We used the simulation benchmarks Spec2017 [23,24] with *ref* inputs. Every benchmark is run as a single-core workload in two different regions of interest: initialization phase and main execution phase (denoted “Init” and “Main,” respectively). Each experiment used 10 billion instructions (both initialization and main execution phases).

B. Experimental Observations of Electromigration Stress

This section examines the EM stress induced by the switching factor in three different parts of the microarchitecture: ALU execution units, architecture register files, and memory hierarchy sub-system. Previous studies ([10, 25] supports our concern that these areas involve the most intensive EM activities when running these workloads and, thus, will experience intense EM stress.

Table 1- Baseline simulation model configuration

Core Model	
Frequency	2.66 GHz
Execution units [time]	3 ALUs [1 cycle], 1 FP add / sub [3 cycles], 1 FP mul / div [5/6 cycles], 1 Branch [1 cycle], 1 Load unit [1 cycle], 1 Store unit [1 cycle]
Pipeline	Dispatch width: 4, Out-of-order (instruction window: 128).
Memory system model	
Block size	64 Bytes
L1-D Cache	32KB, 8-Way, LRU, 4 clock cycles access time and a throughput period of one cycle.
L1-I Cache	32KB, 4-Way, LRU, 4 clock cycles access time with instruction prefetching and instruction queue of 16-byte per cycle throughput
L2 Cache	256KB, 8-Way, LRU, 8 clock cycles access time.
L3 Cache	8MB, 16-Way, LRU, 30 clock cycles access time.
D-TLB	64 entries, 4-Way
I-TLB	128 entries, 4-Way
S-TLB	512 entries, 4-Way (secondary TLB)

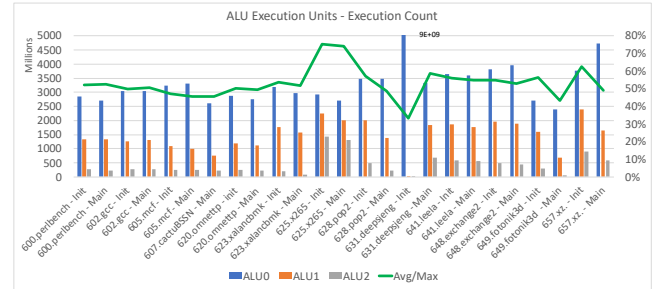


Figure 1- Distribution of ALU execution count

ALUs: Figure 1 shows the distribution of write operations among different ALUs when using the FIFO selection mechanism among all ready-to-execute instructions (all benchmarks were run for 10B instruction so the usage rate per instruction can be easily calculated). Note that ALU0 is the most-used ALU of the three available, and ALU2 is the least used, which is attributed to the fixed allocation policy of the available ALUs, whereby a higher priority is given to an ALU with a lower index. Since ALU execution time is 1 clock cycle, all ALUs become available every cycle. For example, for a program that provides exactly one instruction per cycle, we expect only ALU0 to be used. Figure 1 supports this claim and shows that ALU0 is used at over twice the rate than ALU1, and nearly ten times the rate than ALU2 for most benchmarks. In such a logical implementation, the worst-case switching factor of ALU0 dictates the worst-case EM scenario to be taken into account and applied to all ALUs.

Register-file: Our next set of experiments examines the switching factor on architectural registers. Figure 2 illustrates the distribution of write operations on general-purpose registers (GPRs: integer general purpose) for the Spec2017 benchmarks.

The distribution clearly is not uniform; for example, the RAX register is the most-stressed register in terms of write operations, whereas the non-legacy registers are hardly used and thus are significantly less toggled than the x86 legacy registers. The root cause of these differences is the nature of compiler register-allocation algorithms. Figure 2 also shows that the ratio of the average number of write operations to the maximum number of write operations varies from nearly 7% to 33%. This measurement is another indication that toggle rate is not equally balanced between registers; thus, the register with the greatest number of writes dictates the overall switching ratio for EM.

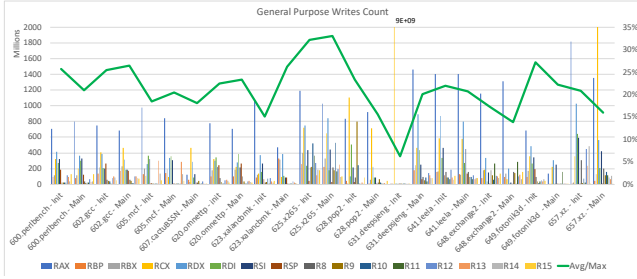


Figure 2 - Distribution of general-purpose-register writes

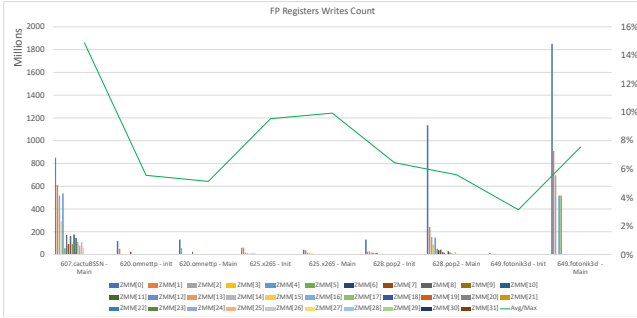


Figure 3 - Distribution of writes to floating point registers

Figure 3 presents the number of write operations on FP registers only for the Spec2017 benchmarks that involve FP operations. The results presented for this case are similar to the results presented in Figure 1. For FP registers, the number of writes is significantly greater in the registers with lower indexes (i.e., ZMM0, ZMM1, and ZMM2 are the registers with the highest write count). Similar to integer registers, this can also be explained by the nature of the register-allocation algorithm of common compilers. In this case, the ratio of the average number of write operations to the maximum number of write operations is even smaller, which is indicative of an even larger variance relative to integer registers.

Memory hierarchy: Memories are highly susceptible to EM because they employ high-density bitcells with narrow and long metal wires that toggle upon every change of logical state. SRAM memories employ lower metal layers for their interconnect, typically, metal 1 – metal 3. As opposed to upper metal layers, the width and height of lower metal layers are significantly smaller and as a result they become highly susceptible to EM stress. In addition, physical design tools lack the ability to handle every bitcell in an individual manner; therefore, the worst-case scenario is commonly applied to all bitcells. Since write operations are not uniformly distributed

across all memory bitcells, the worst-case scenario is determined by the bitcell with the largest number of writes.

Note that the granularity of switching activity differs from one level of memory hierarchy to another; e.g., a single byte can be written in the L1 cache, but a minimum granularity of the cache line is imposed on all other levels of the cache hierarchy (assuming a line-fill mechanism). Since all bits within the write granularity have the same EM stress, we assume that they all have the same probability for failure and therefore conventional error-correction mechanisms may not be effective at that granularity.

We first start our analysis by examining toggle rate of the memory hierarchy elements. Figure 4 shows ratios of the average number of write operations per memory entry. It reveals that DTLB involves significantly more write operations than ITLB. DTLB also involves nearly tenfold more write operations than STLB. A similar observation results from examining the ratio of write access of the L1-D cache to that of the L1-I cache. The L1-I cache involves write operations only upon cache line replacement, whereas L1-D maintains a much higher rate of write operations because of block re-placement and each time an instruction targets a memory location. If we continue examining the write ratios of L1-D to L2 and L2 to L3 then it can be observed that higher level of cache memories experience higher level of toggling rate.

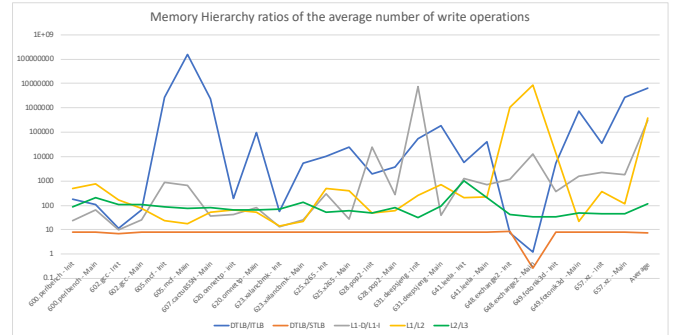


Figure 4 - Write ratios in memory hierarchy

Note that, although the initial observations indicate that the L1-D cache and the D-TLB have the highest write rate, we must still continue carefully watching the write distributions in the remaining memory hierarchy. In particular, it is important to monitor the write distribution to L2 and L3 cache memories. Although our experimental results show that these caches maintain lower write rates, they may be much more susceptible to EM than the L1 caches because of physical design considerations. Since both the L2 and L3 caches are significantly larger than the L1 cache, they involve higher-density memory bitcells and significantly longer and narrower interconnect metal. Equation 2 supports this argument by indicating that the current density is inversely proportional to the metal width and proportional to the wire capacitance. The interconnect metals in both the L2 and L3 caches, which use long wires, introduce a much greater interconnect capacitance than the L1 caches.

Based on this observation, the next graphs focus on how EM affects the L1-D cache, L2 cache, L3 cache, and D-TLB. In the next figures, we present histograms of write operations partitioned into five histogram bins: 0%–25%, 26%–50%,

51%–75%, 76%–90%, and 91%–100%. Each bin shows the number of cache entries with the ratio of write distributions relative to the cache entry with the maximum number of write operations. For example, 20% for bin 26%–50% means that 20% of the cache entries each experienced write operations in a ratio range of 26%–50% relative to the cache entry with the maximum number of write operations. The cache entry with the maximum number of writes is the entry that dictates the EM toggle-rate assumption for the entire cache. Such histograms can help clarify the EM stress distribution among all cache entries and allow us to explore new architecture to relieve EM hotspots.

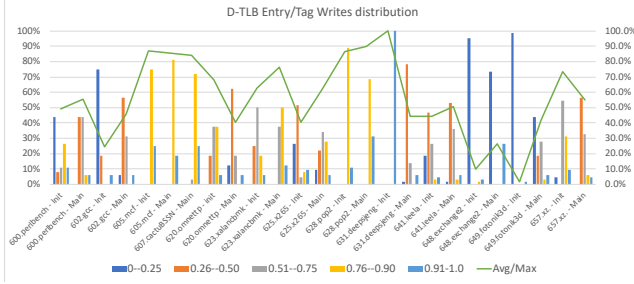


Figure 5 - Distribution of DTLB writes

Figure 5 shows the write histogram of D-TLB entries and their tags. Note that, for all benchmarks, only a small number of entries experience a large ratio (above 90% relative to the entry with the maximum number of writes); these entries dictate the overall switching rate of the D-TLB. The majority of entries experience much lower write rates. Figure 5 also presents the ratio of the average number of writes per entry to the maximum number of writes of all entries, which varies from 2% to 100%, with an average of 55%.

Figure 6 shows a histogram of writes to L1-D cache data lines. A phenomenon appears similar to that observed in the D-TLB. Only a small number of cache lines have a high write ratio (above 90% relative to the maximal data cache line), whereas the majority of cache lines experience much lower write ratios. In most of the benchmarks, the ratio of the average number to the maximum number of writes is less than 30%, whereas the average ratio is 33%.

Figure 7 shows histogram cache writes for the L2 cache data lines. The observations, in this case, are similar to those for the L1-D cache. For both data blocks and tags, we observe that only a small portion of cache entries (data and tags) experience the highest write ratio (>90% relative to the entry with the maximum number of writes) and, as a result, they indicate severe EM conditions for all cache entries. We observe that the ratio of the average number of writes per entry to the maximum number of writes of all entries is approximately 50%. A similar result for write operations on cache lines was also obtained by Valero et al. in their study of the different aspects of cache reliability [19].

Examination of Figure 6 and Figure 7 shows that two benchmarks, 631.deepsjeng-init and 649.fotonik3d-main, behave differently than all other benchmarks. This is explained by the fact that the initialization phase of 631.deepsjeng and the main execution phase of 649.fotonik3d have write distributions that are spread uniformly over most cache lines.

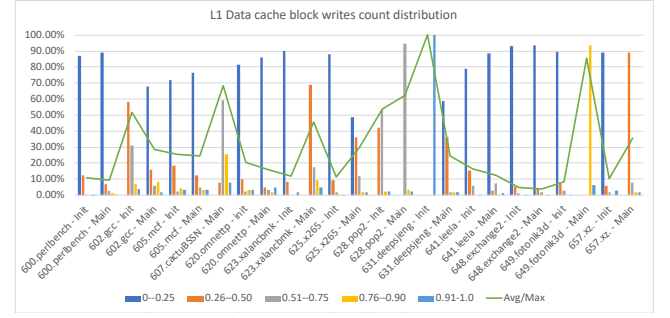


Figure 6 - Distribution of L1-D cache block writes

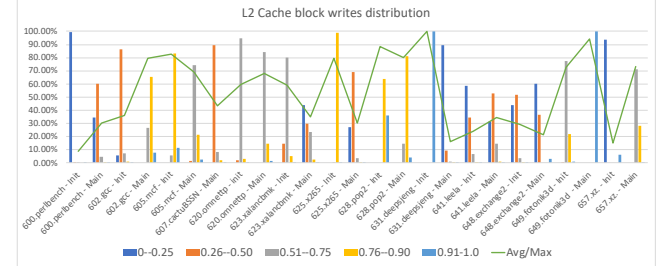


Figure 7 - Distribution of L2 cache block writes

Figure 8 shows a histogram for L3 writes for cache data lines. For most benchmarks, the number of writes is very small for the majority of cache data lines, where almost all of them experience 25% or less write operations relative to a very small portion of cache lines with the maximum number of writes. Overall, the ratio of the average number of write operations to the maximum number of writes is 8%. The benchmark 631.deepsjeng-init behavior in the L3 cache is similar to the behavior of the L2 cache due to the relatively high store instruction count that percolates to the L3 cache.

Figure 9–11 illustrate the write histograms of L1-D, L2, and L3 tag writes, respectively. The tag writes spread more uniformly in compare data lines, and the majority of cache tags experience smaller variance in the number of writes. The ratio of the average number of tag writes to the maximum number of tag writes is nearly 70% on average for the L1-D cache and approximately 50% for L2 and L3 tags.

The results presented in this section, support our observation that cache data lines experience a write distribution with high variance and with a minority of lines being highly stressed by the maximum number of write operations and, as a result, dictate, much more severe EM conditions for the entire cache. Similar conclusions are obtained from our observation of registers write access and ALU use where, in both cases, the EM stress induced by the workload is nonuniformly distributed. Such behavior leads to an over-design condition for EM that can degrade overall performance and increase IC area. In the next section, we propose EM-aware microarchitectural mechanisms to smooth EM stress. This approach results in a dramatic relaxation of the overall EM sign-off design conditions.

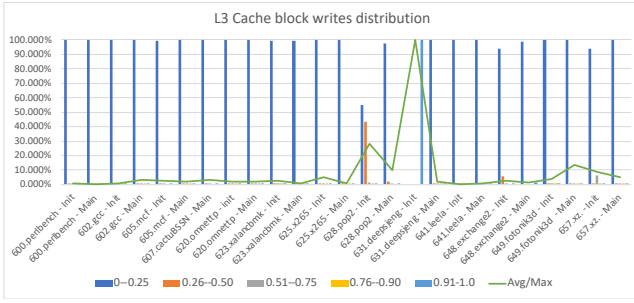


Figure 8 - Distribution of L3 cache block writes

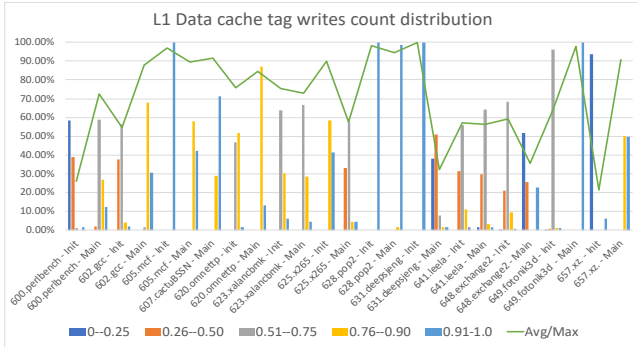


Figure 9 - Distribution of L1-D cache tag writes

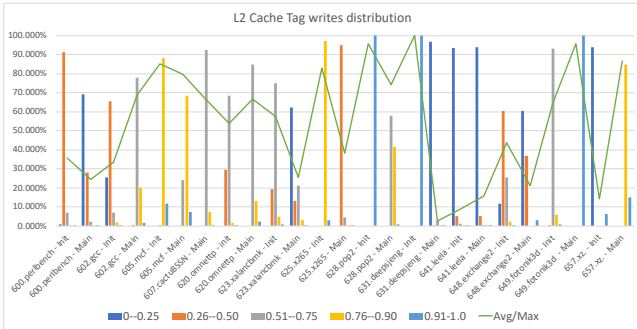


Figure 10 - Distribution of L2 cache tag writes

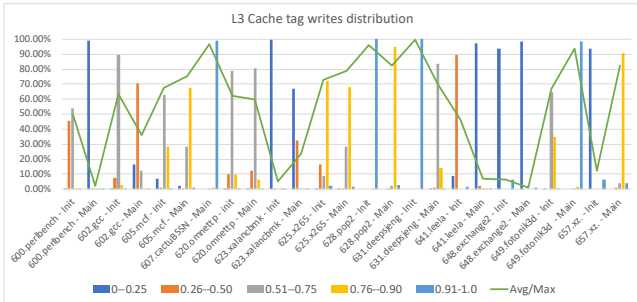


Figure 11 - Distribution of L3 cache tag writes

IV. PROPOSED ELECTROMIGRATION-AWARE RESOURCE-ALLOCATION MECHANISM

This section introduces architecture solutions to reduce EM stress. The principal of the solutions is based on EM-aware resource allocation that smoothens write operations and the use of computational elements distribution over all available resources. As a result, EM stress is significantly reduced. The following subsections introduce EM-aware architectures for dealing with EM stress on ALU execution units, register files, and cache memories, respectively.

A. Electromigration-Aware ALU Allocation

In the previous section, we observed that ALUs are not utilized in an EM-aware manner, which means that the maximum switching activity ratio is dictated by a small, over-used subset of ALUs. The proposed EM-aware scheme assumes that all pending ALU instructions are allocated to a centralized instruction queue, and in each cycle a scheduler allocates ALUs to execution-ready instructions. Although the proposed scheme is described for ALUs, it can also be applied to any type of multi-execution unit employed by microprocessors.

In this study, we present two alternatives that implement the same basic principle in different ways. The aim of both solutions is to start allocating the resources from a different leading point each time. The first simple solution is to have a counter (e.g. 32-bit counter) that is incremented each clock cycle and wraps around when expired so that the leading resource number to use is calculated as counter value modulo the number of physical resources. Thus, for our simulated environment, we assume $N = 3$. When the counter expires, we stop allocating resources for that cycle, reset its content, and continue with the allocation in the next cycle.

The second solution is illustrated in Algorithm 1; here, we extend each resource with a single bit (Ex_counter) and add a single global bit (Global_counter) for the overall management of the allocation. All counters are initialized to zero. We suggest that the EM-aware allocation algorithm selects execution units whose corresponding counter state equals the global counter. If the number of available execution units that satisfy this condition exceeds the required number of instructions to be issued, then a subset (based on the required number of instructions to be issued) of those execution units is selected, and all their corresponding counters are switched (between zero and one). Otherwise, all execution units with their counter state equal to the global counter are selected while the rest of the execution units needed to satisfy the required instruction to be issued are selected from the other pool of ALUs whose counter is not equal to the global counter. In this case, the global counter is incremented. In addition, the counters corresponding to the selected execution units are incremented.

Algorithm 1 – EM-aware execution-unit allocation:

Input: $k < N$ number of execution units to be allocated.

Output: Vector $E = (e_0, e_1, \dots, e_{n-1})$, for every $0 \leq i \leq n-1$, only if $e_i = 1$ execution unit i to be allocated, otherwise not allocated.

Initialization: Ex_counter[i]=0 for every $0 \leq i \leq n-1$, Global_counter=0

1. $M = \{0 \leq i \leq n-1 \mid \text{Ex_counter}[i] = \text{Global_counter}\}$

2. **if** $k < |M|$ **then**

3. let $P \subseteq M$ such that $|P| = k$

4. $e_i = 1$ for every $i \in P$, otherwise $e_i = 0$

5. Ex_counter[i]++ for every $i \in P$

6. **end if**

7. **else** // $k \geq |M|$

8. let $P \subseteq U \setminus M$ such that $|P| = k - |M|$

9. $e_i = 1$ for every $i \in P \cup M$, otherwise $e_i = 0$

10. Ex_counter[i]++ for every $i \in P \cup M$

11. Global_counter++

12. **end else**

13. **return** E

Table 2 shows an example of the algorithm output for three ALUs.

Table 2 - Example of EM-aware ALU scheduling

Clock cycle	Issued instructions	Ex_counter[2:0]	Global counter	Selected ALU(s)
0	0	0, 0, 0	0	None
1	2	0, 1, 1	0	0, 1
2	2	1, 1, 0	1	2, 0
3	3	0, 0, 1	0	1, 2, 0

The implementation of the first solution is straightforward and may perform well given a large number of execution units. The implementation of the second solution is more complicated, but our implementation trial indicates that it can be done with negligible overhead in terms of logical area and computation time for both the ALU-selection logic and the counter-incrementation logic. The following table summarize power, timing and gate count overhead for 28nm process. It should be noted that the proposed solution does not affect timing since the counters are updated in parallel to the ALU execution cycle.

Table 3 - ALU scheduling overhead

	Gate count	Power	Timing impact
Option 1	352	31 nW	None (reg-to-reg delay < clock cycle time)
Option 1/2	292	26 nW	None (reg-to-reg delay < clock cycle time)

B. Electromigration-Aware Registers Allocation

The results of the measurements presented Section 3 clearly indicate that write operations to registers are not uniformly distributed. Moreover, specific registers (e.g., RAX) experienced an excessive number of writes. Such behavior by a small number of registers dictates difficult EM conditions for all registers and may result in reliability concerns. Note that this section deals mainly with architectural registers assigned by the compiler rather than with physical registers implemented by the out-of-order (OoO) microprocessors. For the latter, physical registers are usually implemented as a cyclic buffer within the reorder buffer and, as a result, all writes are spread uniformly over time.

The proposed architectural solution, illustrated in Figure 12, avoids write hotspots in registers by periodically changing the mapping of registers to their corresponding architectural hosting locations. The scheme is based on modulo rotation of the mapping between the architectural register identifier and their physical locations. As illustrated in Figure 12, a pulse trigger is asserted to shift the register mapping in the register-file (RF) either periodically (or each time we change CR3) or as part of the return-from-interrupt procedure before saving the values of the user-level process. A modulo-counter (RF rotator) serves to map the architectural register number to the physical register location by modulo addition. After each assertion of the rotation trigger (at any arbitrary time point), the counter is incremented, and the register values are shifted between registers.

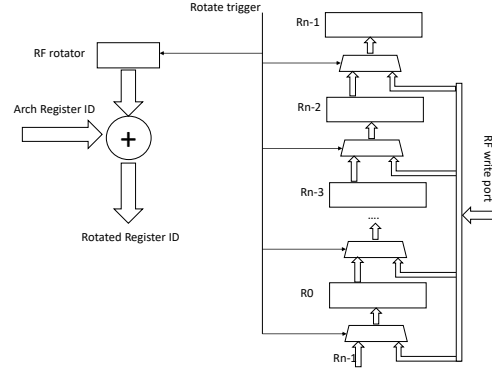


Figure 12 - Scheme for electromigration-aware RF mapping

The following table summarize power, timing path and gate count overhead for 28nm process (for 32 GPRs):

Table 4 - GPR rotation overhead

Gate count	Power	Timing impact
3137	282nW	50ps delay added to access time

The proposed solution has certain similarity to the Sun SPARC and Berkley RISC CPUs register window [26] which is used for different purpose. Register window is a scheme that aims to evenly distribute sets of GPR registers between different sections of code, typically procedure calls, and upon every nested call the register window is shifted to provide the program a new working set of registers. Unlike, the register window technique which is limited to integer registers our proposed scheme is extended to all architectural registers (FP, vector, control etc.). It should also be noted that register window involves more frequent register window switch resulting in excessive dynamic power while the rotation frequency of our proposed scheme is very low.

C. Electromigration-Aware Cache Memories

EM in cache memories generates hot spots in various cache lines that are spread nonuniformly. Note that, in this subsection, the term “cache” refers to any architectural structure that uses a cache organization (e.g., TLBs). As a result, a small fraction of cache lines dictates the worst EM scenario for the entire cache. The principal of the proposed EM-aware cache memory scheme, illustrated in Figure 13, is based on the same principals of the register file solution.

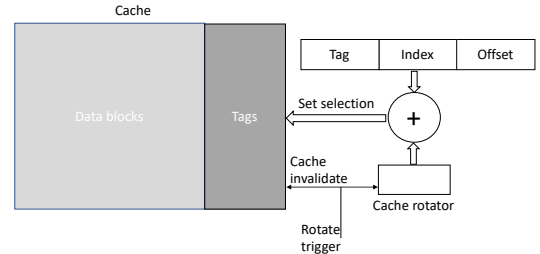


Figure 13 - Electromigration-aware cache memory mapping

Our proposed scheme is similar to two previously introduced solutions for different physical reliability problems.

The first one, introduced by Calimera et al. ([27]) to handle a different problem related to SRAM asymmetric aging, suggested re-indexing cache lines using various mapping function. The second method introduced by Wang et al. ([29]) to mitigate write endurance in PCM based non-volatile memories (NVMs). PCM based NVMs experience bit cell wear out after an excessive number of writes leaving the bitcell resistance in a low or high resistance state. This may happen due to either Ge depletion in the bitcell area or when the heating electrode is detached ([30]). Their proposed technique (similar to Calimera et al.) suggested Swap-Shift method to swap a pair of cache sets whenever a number of writes reaches a certain threshold. By using similar technique, our proposed scheme avoids hotspots of cache writes by periodically changing the cache set mapping of memory addresses to their corresponding physical cache lines. As with the RF solution, the principal of this scheme is based on modulo rotation of the mapping between the set field (taken from the memory address) and its physical set location. A pulse trigger is periodically asserted to shift the mapping of the set. A modulo-counter (cache rotator) maps the address set field to the physical set location by modulo addition. After each assertion of the rotation trigger, the counter is incremented, and all cache lines are invalidated. The following table summarize the power, critical timing path impact and gate count overhead for 28nm process:

Table 5 - Cache rotator overhead

Cache index size	Gate count	Power	Timing impact Delay added to access time
6 bits (L1-D)	89	8nW	60ps
7 bits (L1-I)	114	10.2nW	63ps
9 bits (L2)	173	15.6nW	67ps
13 bits (L3)	327	29.5nW	76ps

To avoid the potential overhead incurred by flushing the caches content (and by the write-back of all the dirty lines), we suggest doing the operation either very infrequently or by exploiting events that require flushing these structures (e.g., after a sleep mode when all caches were cleaned).

V. EXPERIMENTAL STUDY OF ELECTROMIGRATION-AWARE ARCHITECTURE

This section presents the experimental results for the proposed architecture solution (presented in the previous section) to reduce the impact of EM. The metric that we use to quantify our EM stress reduction is defined as follows:

$$EM \text{ Stress Reduction} = 1 - \frac{P_{\max EM\text{-aware}}}{P_{\max original}}$$

Equation 3 - EM Stress Reduction

where $P_{\max EM\text{-aware}}$ and $P_{\max original}$ are the maximum toggle rates of a module with EM-aware architecture and the original architecture respectively. In addition, the metric of MTTF improvement is defined as the ratio of the EM-aware MTTF to the original MTTF and by applying Equations 1-3 the following equation is obtained:

$$MTTF \text{ improvement} = \frac{1}{1 - EM \text{ Stress reduction}}$$

Equation 4 - MTTF Improvement

Note that our proposed techniques in Section 4 did not report performance overhead, so this section focuses on how the algorithms proposed herein affect the EM stress. We first examine an EM-aware solution for ALU execution units. Figure 14 shows how the second solution presented in the previous section (see Algorithm 1) affects the EM stress for the SPEC2017 benchmarks. Examination of the two solutions indicates that they behave very similarly. The results show that the proposed algorithm significantly reduces EM stress by 50% over all benchmarks. The results vary from nearly 25% reduction up to 65% reduction. This result is because the proposed scheme distributes ALU use uniformly and reduces the maximum EM stress.

As part of this study, we also compare the instructions per cycle (IPC) versus EM stress reduction, as shown in Figure 15. Benchmarks with small IPC have a greater potential for EM stress reduction because of the underused ALUs that could potentially help reduce the maximum EM hotspots.

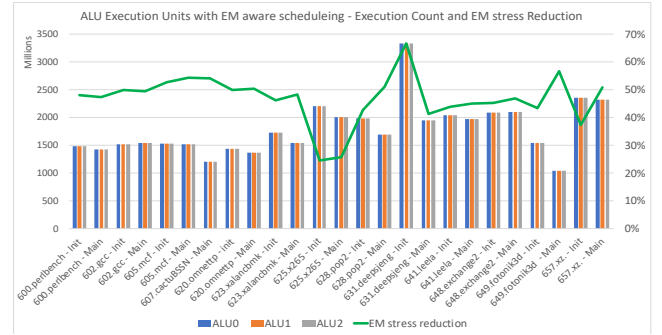


Figure 14 - Distribution of ALU execution count with electromigration-aware allocation

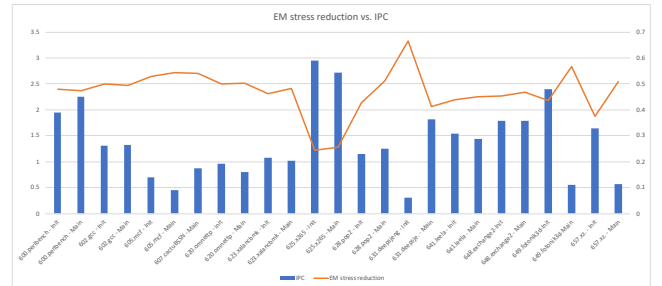


Figure 15 - ALU electromigration stress reduction vs. IPC

The next results show the EM stress reduction obtained by the proposed architectural solution for both the GPR register file and FP register file (Figure 16 and Figure 17, respectively). For both register files, the number of writes is distributed uniformly over all registers, and no hotspots exist. In addition, the write stress decreases dramatically by nearly 80% on average for the GPR registers and 90% for the FP registers. The rotation trigger in the simulation was asserted every 10 million clock cycles. We examined different rotation trigger rates and found that this value does not impact performance.

As part of the experiments, we also observed that the flags and stack-pointer registers experienced excessive stress of write

operations, which makes them highly susceptible to EM stress. Figure 18 illustrates the number of write operations to the flags register and stack-pointer register and compares them with the maximum number of writes per register in the GPR register file. For almost all benchmarks, the number of writes to the flags register significantly exceeds those to the GPR and stack-pointer registers. This result is due to the fact that almost every instruction involves implicit write to the flag register, which motivates us to extend the EM-aware scheme proposed for the GPR register file to include both the flag and stack-pointer registers. Figure 18 shows that, in this case, the maximum number of write operations is reduced even more (varying from 80% to >90%).

The last part of this section is devoted to examining the reduced EM stress for the TLBs and cache data lines and tags. The results are illustrated in Figure 19 and Figure 20, respectively. In most cases, the EM stress is significantly reduced as a result of the repetitive rotation of the set mapping and invalidation. This helps to distribute write operations uniformly over all sets and ways. For the D-TLB, we suggest triggering the rotation either when the TLB is flushed by the system, or by performing a period rotation (e.g., every 10M TLB accesses). For the L1-D cache, we suggest a similar periodic rotation trigger every 10M accesses. For all these options, the performance overhead is minimal. As previously discussed, for both L2 and L3, we suggest triggering the set rotation upon each system wakeup from sleep mode. In this case, no performance overhead is incurred. In our simulation we use an interval of 10M cache accesses, the same trigger duration of the L1-D cache for both the L2 and L3 caches.

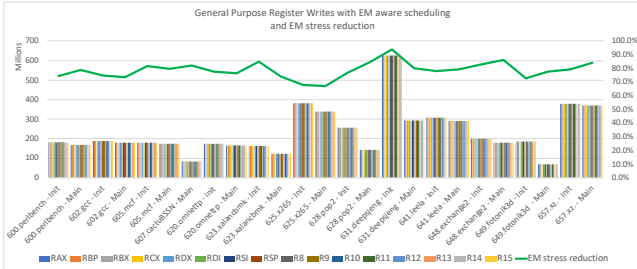


Figure 16 - GPR writes distribution with EM-aware allocation

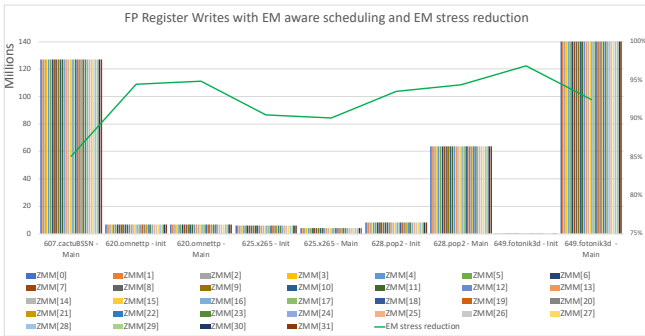


Figure 17 - FP register writes distribution with EM-aware allocation

Figure 19 illustrates the write-stress reduction for DTLB. On average, the stress is reduced by 44% over all benchmarks. Figure 19 also summarizes the EM stress reduction for L1-D, L2, and L3 caches. For L1-D, L2, and L3 caches an average reduction in the maximum number of writes is 69%, 46%, and

92%, respectively. Figure 20 summarizes the EM stress reduction in cache tags. In this case, the reduction is 28%, 46%, and 46% for L1-D, L2, and L3 caches, respectively. Note that the experimental results of the EM-aware architectural solution are consistent with the results presented in Section 3. These figures suggest that a smaller ratio of the average number of write operations to the maximum number of writes corresponds to greater EM stress reduction.

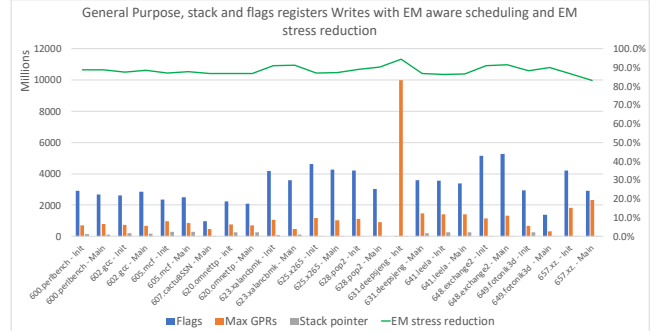


Figure 18 - Distribution of GPRs, flags, and stack pointer writes with EM-aware allocation

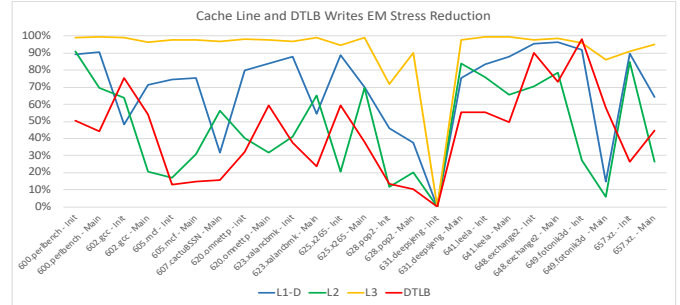


Figure 19 - Cache lines electromigration stress reduction

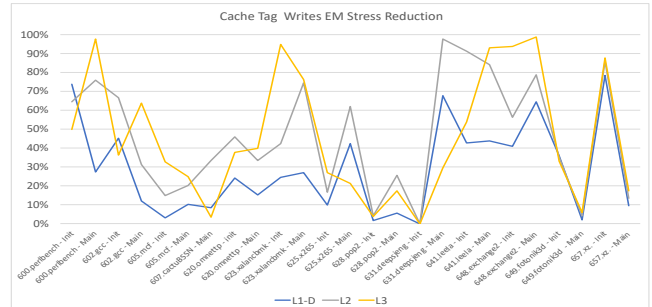


Figure 20 - Cache tags electromigration stress reduction

Based on the experimental results, we observe that EM stress can be significantly reduced in the microprocess building blocks that are examined. The observations detailed herein reveal an average reduction in EM stress of 50% for ALUs, 80%–90% for the register files, and 46%–92% for cache data blocks. These results indicate that the proposed EM-aware solution should allow microprocessor designers to significantly relax the maximum toggling rate and, as a result, to avoid a significant number of potential EM violations.

Alternatively, the reduction in the maximum switching rate translates into an extended device lifetime. As indicated in Section 2, the MTTF is proportional to the switching rate, so a reduction of 50% in the switching rate should double the

lifetime. These numbers, of course, depend on the workload being run by the microprocessor, and benchmarks exist where EM stress is reduced even more (e.g., in 600.perlbench the write reduction in the memory hierarchy exceeds 70%, which may more than triple the overall lifetime). Still, a small number of benchmarks exist with less EM stress reduction (e.g., 628.pop2, for which the EM stress reduction is 5%–25%). As a result, the overall gain in lifetime is 5%–33%.

VI. CONCLUSIONS

Microprocessor reliability is a crucial requirement that introduces major micro-architectural and design challenges. Traditionally, reliability and EM related issues are handled at the physical design level that enforces design rules using worst case scenario analysis in order to detect violations and attempts to solve them. Contrarily, our study presented EM-aware micro-architectural solution that can significantly relax the over-design of traditional methods and extend the lifetime of microprocessors by more than double.

This paper indicates that microprocessors are highly susceptible to EM because they process highly variable dynamic workloads on non-EM-aware micro-architectures. We introduce herein an architectural solution that takes into account the EM effect and reduces excess use of execution units and write operations to registers and memory-hierarchy elements. The principal of the proposed solution is based on EM-aware resource allocation that attempts to uniformly distribute write operations and the use of computational elements over all available resources. Our analysis shows that the proposed solutions incur minor area and power overhead and negligible performance degradation. In addition, our experimental results indicate that the proposed architecture significantly relaxes the EM sign-off conditions by 50% for ALUs, 80%–90% for the register files, and 46%–92% for the data blocks of cache memories. Since the MTTF is proportional to the switching rate, these results translate to at least a twofold extension in lifetime. This, of course, depends on the specific workload; for certain benchmarks, the lifetime extension may be threefold or even higher.

EM has become a major challenge in advanced technologies, and further studies are required to continue exploring new architectures and to identify other avenues to reduce EM and extend device lifetime. In this study, we examined how EM stress affects modern microprocessors, although the approach used herein may be extended to other processing elements such as VLIW machines, security engines, GPUs, and TPUs. We also encourage future studies to examine software-based solutions for EM stress reduction to avoid EM hotspots.

REFERENCES

- [1] [1] X. Xuan, Analysis and Design of Reliable Mixed-Signal CMOS Circuits, PhD thesis, Georgia Inst. of Technology, Dept. of Electrical and Computer Engineering, 2004.
- [2] [2] J. Lienig and G. Jerke, Embedded Tutorial: Electromigration-Aware Physical Design of Integrated Circuits, Proc. 18th Int'l Conf. VLSI Design (VLSID 05), IEEE Press, 2005, pp. 77–82.
- [3] [3] J. Lienig, Introduction to electromigration-aware physical design. In Proceedings of the International Symposium on Physical Design (ISPD'06). ACM, New York, 39–46.
- [4] [4] J. Lienig, Electromigration and Its Impact on Physical Design in Future Technologies. Proceedings of the 2013 ACM International symposium on Physical Design, March 2013.
- [5] [5] J. Srinivasan, S. V. Adve, P. Bose and J. A. Rivers. Lifetime Reliability: Toward an Architectural Solution. IEEE Micro, special issue on Emerging Trends, vol. 25, issue 3, May–June 2005, 2–12.
- [6] [6] J. Srinivasan, S. V. Adve, P. Bose and J. A. Rivers. Exploiting Structural Duplication for Lifetime Reliability Enhancement. the Proceedings of the 32nd International Symposium on Computer Architecture (ISCA'05) June 2005.
- [7] [7] A. Dasgupta and R. Karri, Electromigration Reliability Enhancement Via Bus Activity Distribution, Proc. 33rd Ann. Conf. Design Automation (DAC 96), ACM Press, 1996, pp. 353–356.
- [8] [8] J. Abella, Xavier Vera, Osman S. Unsal Oguz Ergin, Antonio Gonzalez and James W. Tschanz. Refueling: Preventing Wire Degradation due to Electromigration. IEEE Micro (Volume: 28 , Issue: 6 , Nov.-Dec. 2008).
- [9] [9] J. Tao et al., Modeling and Characterization of Electromigration Failures under Bidirectional Current Stress, IEEE Trans. Electron Devices, vol. 43, no. 5, May 1996, pp. 800–808.
- [10] [10] J. Abella and X. Vera, Electromigration for Microarchitects. ACM Computing Surveys (CSUR) March 2010 Article No.: 9
- [11] [11] Operating Temperature, Wikipedia - https://en.wikipedia.org/wiki/Operating_temperature.
- [12] [12] Failure Mechanism based Stress test Qualification for Integrated Circuit. Automotive Electronics Council, Component Technical Committee - AEC - Q100 - REV-G standard.
- [13] [13] J. R. Black, "Electromigration – A brief survey and some recent results," IEEE Trans. on Electronic Devices (April 1969), 338–347. DOI= <http://dx.doi.org/10.1109/T-ED.1969.16754>
- [14] [14] Andrew B. Kahng, Siddhartha Nath and Tajana S. Rosing, On Potential Design Impacts of Electromigration Awareness. 2013 18th Asia and South Pacific Design Automation Conference (ASP-DAC)
- [15] [15] I. A. Blech, Electromigration in thin aluminum films on titanium nitride, J. Appl. Phys., vol. 47 (1976), 1203–1208. <http://dx.doi.org/10.1063/1.322842>
- [16] [16] C. S. Hau-Riege, An introduction to Cu electromigration, Microel. Reliab., vol. 44 (2004), 195–205. DOI= <http://dx.doi.org/10.1016/j.microrel.2003.10.020>
- [17] [17] A. Scorzoni, B. Neri, C. Caprile, F. Fantini, Electromigration in thin-film inter-connection lines: models, methods and results, Material Science Reports, New York: Elsevier, vol. 7 (1991), 143–219. [http://dx.doi.org/10.1016/0920-2307\(91\)90005-8](http://dx.doi.org/10.1016/0920-2307(91)90005-8)
- [18] [18] D. Young, A. Christou, Failure mechanism models for electromigration, IEEE Trans. on Reliability, vol. 43(2) (June 1994), 186–192. DOI= <http://dx.doi.org/10.1109/24.294986>
- [19] [19] A. Valero, N. Miralaei, S. Petit, J. Sahuquillo, and T. M. Jones. On Microarchitectural Mechanisms for Cache Wearout Reduction. IEEE Transactions on Very Large-Scale Integration (VLSI) Systems, Vol. 25, No. 3, March 2017.
- [20] [20] J. Srinivasan, S. V. Adve, P. Bose and J. A. Rivers, The Case for Lifetime Reliability-Aware Microprocessors, Proceedings of 31st International Symposium on Computer Architecture (ISCA '04) June 2004.
- [21] [21] T. E. Carlson, W. Heirman, and L. Eeckhout. Sniper: Exploring the level of abstraction for scalable and accurate parallel multi-core simulations. In Proceedings of the International Conference for High Performance Computing, Networking, Storage and Analysis (SC), Nov. 2011.
- [22] [22] M. E. Thomadakis. The architecture of the Nehalem processor and Nehalem-EP smp platforms. Technical report, December 2010. <http://sc.tamu.edu/systems/eos/nehalem.pdf>.

- [23] [23] A. Limaye and T. Adegbiya, "A workload characterization of the spec cpu2017 benchmark suite," in 2018 IEEE International Symposium on Performance Analysis of Systems and Software (ISPASS), pp. 149–158, April 2018
- [24] [24] Q. Wu, Steven Flolid, Shuang Song, Junyong Deng, Lizy K. John. Hot Regions in SPEC CPU2017. 2018 IEEE International Symposium on Workload Characterization (IISWC).
- [25] [25] K-T Jang, Y-J Park, MW Jeong, S-M Lim, H-W Yeon, J-Y Cho, M-G Jin, J-S Shin, B-W Woo, J-Y Bae, Y-C Hwang, Y-C Joo. Electromigration behavior of advanced metallization on the structural effects for memory devices. Microelectronic Engineering Volume 156, 20 April 2016, Pages 97-102
- [26] [26] The SPARC Architecture Manual, Version 8.
- [27] [27] A. Calimera, M. Loghi, E. Macii and M. Poncino, "Dynamic Indexing: Leakage-Aging Co-Optimization for Caches," in IEEE Transactions on Computer-Aided Design of Integrated Circuits and Systems, vol. 33, no. 2, pp. 251-264, Feb. 2014, doi: 10.1109/TCAD.2013.2287187
- [28] [28] K. Swaminathan, N. Chandramoorthy, C. Cher, R. Bertran, A. Buyuktosunoglu and P. Bose, "BRAVO: Balanced Reliability-Aware Voltage Optimization," 2017 IEEE International Symposium on High Performance Computer Architecture (HPCA), Austin, TX, 2017, pp. 97-108, doi: 10.1109/HPCA.2017.56.
- [29] [29] J. Wang, X. Dong, Y. Xie and N. P. Jouppi, "i2WAP: Improving non-volatile cache lifetime by reducing inter- and intra-set write variations," 2013 IEEE 19th International Symposium on High Performance Computer Architecture (HPCA), Shenzhen, 2013, pp. 234-245, doi: 10.1109/HPCA.2013.6522322.
- [30] [30] Mohammad Khavari Tavana, Amir Kavyan Ziabari, Mohammad Arjomand, Mahmut Kandemir, Chita Das, and David Kaeli. 2017. REMAP: a reliability/endurance mechanism for advancing PCM. In Proceedings of the International Symposium on Memory Systems (MEMSYS '17). Association for Computing Machinery, New York, NY, USA, 385–398. DOI:<https://doi.org/10.1145/3132402.3132421>



Freddy Gabbay graduated his B.Sc. (summa cum laude), M.Sc. and Ph.D. at the EE department of the Technion - Israel Institute of Technology, Haifa, Israel in 1994, 1995 and 1998 respectively. His areas of research are HPC accelerators, VLSI design, chip reliability, microprocessor architecture and machine learning.

In 1998, he worked as a researcher at Intel Micro-processor Research Lab. In 1999 he joined Mellanox Technologies and held various positions in leading various product lines architecture and ASIC design. In 2003, he joined Freescale Semiconductor as a senior design manager and led the baseband ASIC products. In 2012 he joined back Mellanox Technologies where he served as Vice President of Chip Design.

Today he is an Associate Professor at the Ruppin, Academic Center, Israel. Prof. Gabbay also holds 19 patents.



Avi Mendelson is a visiting professor at the CS and EE departments at the Technion, Israel Institute of Technology, Haifa, Israel and in the EE department, NTU, Singapore. He has a blend of industrial and academic experience in several different areas such as Computer architecture, Power management, security, and Real-Time Systems.

As part of his industrial role, he worked for National semiconductor, in the team that invented and developed the first PC-on-the-Chip. At Intel he worked 5 years as a researcher in Intel research labs and 6 years as principle engineer in the mobile CPU architecture team where he was chief architecture of the first CMP feature (multicore) of Intel cores. For this task and leadership, he got the IAA (Intel Achievement Award)

Prof. Avi Mendelson is IEEE Fellow, was a member of the Board of Governors of the IEEE Computer Society and served as a second VP of the IEEE computer Society.